Disordered Photonic Time Crystals

Yonatan Sharabi, Eran Lustig, and Mordechai Segev*
Solid State Institute, Technion—Israel Institute of Technology, Haifa 32000, Israel

(Received 22 November 2020; accepted 3 March 2021; published 23 April 2021)

We study the propagation of electromagnetic waves in disordered photonic time crystals: spatially homogenous media whose refractive index changes randomly in time. We find that the group velocity of a pulse propagating in such media decreases exponentially, eventually coming to a complete stop, while experiencing exponential growth in intensity. These effects greatly depend on the Floquet band structure of the photonic time crystal, with the strongest sensitivity to disorder occurring in superluminal modes. Finally, we analyze the ensemble statistics and find them to coincide with those of Anderson localization, exhibiting single parameter scaling.

DOI: 10.1103/PhysRevLett.126.163902

A photonic time crystal (PTC) is a spatially homogeneous medium with a refractive index varying periodically in time, $n(t)$ [1]. It was shown [2–6] that a temporal change in the wave impedance causes temporal reflection and refraction for any wave propagating within the time-varying medium. Such time reflections become dominant when the temporal change is both fast (on the timescale of the cycle of the wave propagating in the medium) and strong (refractive index change on the order of at least ~0.1). The time-reflected waves interfere with one another, and if the temporal modulation is periodic, the interference gives rise to Floquet modes with a band structure in momentum space [7–9] and topological properties [10,11]. In one spatial dimension (1D), PTCs seem to be the temporal analogue of 1D photonic crystals. However, despite the similarity, PTCs are profoundly different from (spatial) photonic crystals. First, PTCs—being spatially homogeneous—conserve momentum, whereas dielectric photonic crystals conserve energy. Second, PTCs display momentum band gaps [8–10,12], rather than the energy gaps in photonic crystals. Fundamentally, the differences between PTCs and spatial photonic crystal arise from the arrow of time. Namely, while Bragg reflection from a spatial 1D lattice deflects the wave in space, for PTCs, a temporal change in permittivity cannot cause backreflection in time (unfortunately, for mankind); rather, causality implies that the time reflection also occurs in space. Thus far, PTCs have been demonstrated only in transmission lines [9]. However, recent advances with nonlinear effects in epsilon-near-zero materials [13] have enabled very large femtosecond variations in the refractive index on the order of ~1 [14,15] and the observation of time refraction [16,17]. With these in mind, studying electromagnetic (EM) waves in photonic time crystals is becoming accessible to experiments.

PTCs, the temporal analogue of photonic crystals, are periodic by definition, but many wave systems are not completely periodic and contain an element of disorder. The dynamics of waves in disordered media have been a major research topic since Anderson suggested that scattering from disorder can bring transport to a halt [18]. Localization is now known to be a ubiquitous wave phenomenon occurring for EM waves [19–24], acoustic waves [25], cold atoms [26], and other wave systems. Optics, specifically, became a popular experimental platform for studying Anderson localization due to the non-interacting nature of photons and the long coherence times [27]. An important prerequisite for Anderson localization is that the disorder remains constant (frozen) in time. For years, it was believed that waves in systems that vary in time, even if they remain spatially disordered at all times, are not only nonlocalized [28], but can even display hypertransport [29,30]. However, this view was changed by a recent suggestion that a time-varying system modulated by a properly disordered pseudoperiodic driving force may display localization in the time domain [31–33]. These studies examined a spatially periodic system governed by the Schrödinger equation and found that its Floquet eigenmodes are localized in space and periodic in time. However, those dynamic disordered systems were studied in the context of the Schrödinger equation, where time reflections are impossible; i.e., the temporal dynamics are described by the first derivative of the wave function. In sharp contrast, systems governed by a wave equation with a second derivative in time, such as Maxwell's equations, do allow time reflections and therefore enable a plethora of phenomena, many of them completely new [34]. One important manifestation of such fast variations is the PTCs described above.

The similarities and differences between PTCs and spatial photonic crystals raise fundamental questions regarding waves in PTCs containing disorder: Will such waves localize, as waves in a disordered photonic crystal do, or will we witness new phenomena? Will an optical

pulse launched into a disordered PTC undergo complete reflection, as its spatial analogue does, or will the fundamental difference between time and space result in different dynamics?

Here, we study the dynamics of light propagating in disordered PTCs—PTCs to which random fluctuations are added. We find that the velocity of a pulse propagating in a disordered PTC slows down exponentially once the temporal disorder begins, eventually coming to a complete stop. The dynamics and the slowing down rate depend on the specific band structure of the PTC and the momentum spectrum of the pulse. In contrast to Anderson localization, here, the amplitude of the pulse grows exponentially, and the modes with the highest group velocity are the most susceptible to disorder, displaying the greatest deceleration. Finally, we examine the ensemble statistics of waves in disordered PTCs and underpin the similarities and differences with Anderson localization including single parameter scaling. Conceptually, the results presented here are not restricted to the realm of PTCs, but rather apply to all wave systems that include a second time derivative and therefore experience time reflection, such as acoustics, water waves [6], and other classical wave systems.

We begin by considering a laser pulse propagating in a spatially homogeneous medium whose refractive index varies in time. Figure 1(a) illustrates a Gaussian pulse (blue), which is entirely contained in the medium (gray) and propagating within it. Consider now what happens when the medium changes its properties in time, due to an external force acting on it, such as time-dependent stress or an external high intensity light pulse inducing permittivity change.

The EM waves inside the medium experience time reflection and refraction when a temporal change occurs. Let us assume that the temporal permittivity variations are abrupt, occurring in time segments, as illustrated in Fig. 1(b). As shown in [35], for such a temporal boundary, the reflection and transmission (for D) are

$$r = (Z_1 - Z_2)/2Z_1, \qquad t = (Z_2 + Z_1)/2Z_1,$$
$$Z_i = D_i/B_i = \sqrt{\varepsilon_i/\mu_i}, \tag{1}$$

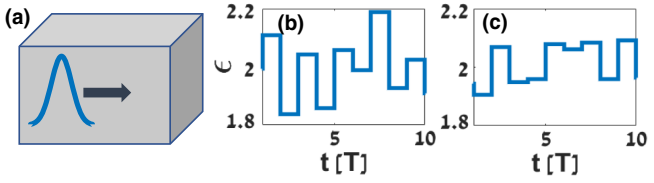

FIG. 1. (a) Gaussian light pulse propagating in the spatially homogenous medium of a disordered PTC. The pulse is fully contained within the PTC. (b),(c) Time-dependent permittivity in a single realization of a disordered PTC showing the time segments of equal duration T, under disorder magnitude $A = 0.1$, (b) with and (c) without, underlying periodicity.

where Z_i is the wave impedance in temporal segment i [36]. Consider a plane wave with wave number k of the form $D(t,z) = D_0 \exp[i(\omega_1 t - kz)]\hat{x}$ propagating in a medium with ε_1, μ_1 (where $k = \omega\sqrt{\varepsilon_1\mu_1}$). At some point in time, the parameters of the medium change abruptly to ε_2, μ_2. This temporal interface results in two plane waves: the transmitted wave $D_t(t,z) = tD_0 \exp[i(\omega_2 t - kz)]\hat{x}$ propagating in the same direction, and the backreflected wave $D_r(t,z) = rD_0 \exp[i(\omega_2 t + kz)]\hat{x}$ propagating in the opposite direction (but not reflected back in time), with $\omega_2\sqrt{\varepsilon_2\mu_2} = k$. Because of the translational symmetry (the medium is spatially homogenous at all times), the momentum is conserved; thus k is conserved through all temporal changes. On the other hand, the frequency ω changes with each temporal change of parameters, to fulfill the dispersion relation $\omega\sqrt{\varepsilon\mu} = k$. The temporal variations (induced by the external force) change the EM energy density stored within the medium. If the variations are periodic, $\varepsilon(t) = \varepsilon(t+T)$, the cumulative effect of time reflections and refractions form a PTC, endowed with bands and band gaps in momentum. This raises the question, what will be the cumulative effect of such time reflections when they are random?

For simplicity, we study here a binary PTC comprised of equal "time segments," each lasting T, corresponding to a modulation frequency of $\Omega = 2\pi/T$ (the permittivity function, however, has an infinite spectrum of frequencies). This binary PTC has ambient permittivity of 2 with a periodic modulation of magnitude 0.1, resulting in two alternating segments with permittivities $\varepsilon_1 = 1.9$, $\varepsilon_2 = 2.1$. On top of this periodic variation, for each time segment, we add a random value, drawn from $\Delta\varepsilon = A \times U[-1,1]$, with A indicating the disorder magnitude and $U[-1,1]$ describing uniform distribution. An example of one such realization of temporal disorder is sketched in Fig. 1(b), showing the permittivity $\varepsilon(t)$ in a disordered PTC. During each segment, the permittivity is constant, but with an abrupt change at the boundary between segments. Such disordered PTCs are a temporal analogue of a disordered multilayer medium, i.e., a one-dimensional photonic crystal.

To understand the dynamics of a light pulse in such a disordered PTC, we simulate the system using finite-difference time domain simulations adjusted to include the temporal variations. In addition, we verify our results, using spectral decomposition analysis, where we decompose the pulse to its momentum components, evolve each one of them in time, and recombine them at each time point. In random disordered systems such as ours, it is necessary to use a large ensemble of disorder realizations and calculate the mean value for each feature [24]. Through such ensemble averaging, we reveal the characteristic behavior of the system as a whole. In our simulations here, we use an ensemble of 10^5 realizations for each data point in our figures.

We begin by studying the simplest form of a temporally disordered medium: the case where no periodic modulation exists and both segments of the PTC have the same permittivity value, to which disorder is added. This system forms a temporally disordered dielectric medium with no underlying temporal periodicity (this is, in fact, not even an actual PTC, since it has no underlying periodicity):$\varepsilon = 2 + A \times U[-1, 1]$. An example of one realization is shown in Fig. 1(c). Here, the pulses have $200T$ FWHM and central frequency of $\Omega/5$, propagating in a homogenous medium with relative permittivity of $\varepsilon = 2$, until at $t = 0$, temporal disorder begins with $\varepsilon = 2 + A \times U[-1, 1]$.

We find that, as the pulse propagates in the temporally disordered medium, its velocity decreases, its energy grows, and its shape is distorted. This is a direct result of the random time reflections it experiences. An example of a pulse envelope evolving in a single disorder realization is shown in Fig. 2(a), demonstrating how its envelope changes after propagating for $2000T$. Figures 2(b) and 2(c) show the mean pulse group velocity and the mean pulse energy, respectively, both calculated from ensemble average. To highlight the specific effects the temporal disorder has on the pulse, we compare three different cases with different disorder magnitudes. The first system is the trivial case in which A, the disorder magnitude, is zero (blue plots in Fig. 2), representing ordinary propagation in a time-invariant homogeneous medium. In the second case, we introduce temporal disorder of low magnitude, $A = 0.1$ (red plots in Fig. 2). And in the third case, we increase the magnitude of the temporal disorder to $A = 0.25$ (yellow plots in Fig. 2).

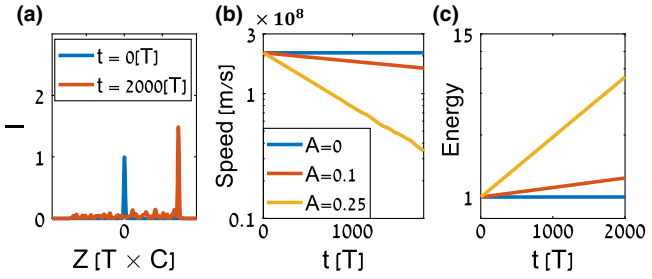

FIG. 2. Pulse propagation in a temporally disordered medium without underlying temporal periodicity. (a) A single disorder realization, displaying the pulse envelope just before the disorder begins ($t = 0$, blue) and after propagating $2000T$ (red, $A = 0.25$). The temporal disorder slows the pulse, increases the amplitude, and causes ripples is the trailing tail. (b) Group velocity of the pulse (log scale) as a function of time. In the system with no modulation (blue), the velocity remains constant. In the system with low disorder magnitude (red), the velocity decays exponentially to zero. In the system with high disorder magnitude (yellow), the decay is steeper. (c) Pulse energy as a function of time. The system with no modulation (blue) conserves the pulse energy, while in the systems with temporal disorder (red and yellow) the pulse energy grows exponentially, with a faster rate when the disorder magnitude is larger (yellow).

We find that once the temporal disorder begins, the mean group velocity of the pulse (calculated from center of mass) decreases exponentially to zero, and the exponential decay becomes steeper as the disorder magnitude increases. These results are shown in Fig. 2(b), displaying the mean group velocity of pulses propagating in the three systems: $A = 0$ in blue, $A = 0.1$ in red, and $A = 0.25$ in yellow.

Next, we examine the pulse energy as a function of time [Fig. 2(c)]. For the system with no disorder (blue), we again find ordinary propagation with the pulse energy remaining constant. In the disordered systems (yellow and red), we find exponential growth of the pulse energy, as indicated by the linear growth in the log-scale plots in Fig. 2(c), with the faster growth in the system with the stronger disorder ($A = 0.25$, yellow).

Up to this point, we examined the simple case of temporal disorder with no underlying time periodicity, thus leaving out the effects of the PTC band structure. We now move on to study the more interesting case of disordered PTCs. We find that localization in temporally disordered PTCs is related to Anderson localization in 1D spatially periodic systems, but also displays some important differences. Generally, the light pulses in the disordered PTCs slow down exponentially, and their amplitude grows accordingly, but the potency of these effects greatly depends on the PTC band structure as we explain next.

Let us first recall some features of Anderson localization in spatially disordered 1D systems. When disorder is introduced into a 1D system, all waves become localized with exponentially decaying tails, and all wave packets come to a complete halt. However, dispersion (effective mass) has a profound impact. In spatially periodic systems, the group velocity is proportional to the $\partial\omega/\partial k$ relation derived from the band structure and generally drops to zero at the band edges. In spatially periodic systems containing disorder, the modes on the band edge, which also have the lowest group velocity, are the most susceptible to disorder and are the first to become localized [37]. The wave functions of these band-edge modes also exhibit the steepest exponential decay (described by the Lyapunov exponent) [21,38]. Following similar logic, we find that in a disordered PTC, the effects of disorder are also dependent on the band structure, with the modes on the band edge being the most susceptible to it. Interestingly, in PTCs, these modes on the band edges are the ones with the highest group velocity, which can even be superluminal (the information velocity, however, is of course not superluminal). Nevertheless, despite their high group velocity, the band-edge modes are the first to slow down and their wave functions display the steepest exponential growth. This phenomenon is shown in Fig. 3, where we simulate pulse propagation for $200T$, at the edge of the first band of the PTC, the region where the variation in the group velocity is the steepest. In this example, the unit cell of the PTC consists of two time segments of equal duration

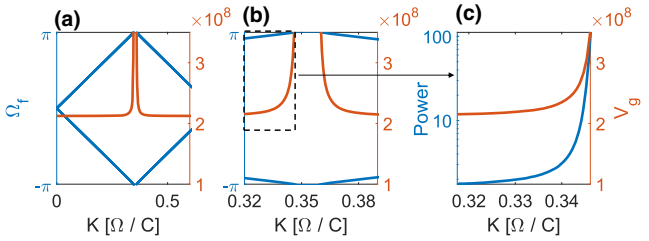

FIG. 3. (a) Band structure of a PTC without disorder, displaying the two momentum bands (blue) and band gaps as well as the corresponding group velocity (red). (b) Same as (a) with a focus on the band gap region. The PTC band structure (blue) and the group velocity (red) on the two band edges, clearly display a band gap at 0.35–0.36$[\Omega/c]$. (c) Enlargement of the dashed region of (b) highlighting just the first (left) band edge, showing the group velocity (red) and the power increase of each momentum component after propagating for $200T$ in log scale (blue). The closer the momenta are to the edge, the higher the group velocity, and therefore the larger the exponential growth in that region.

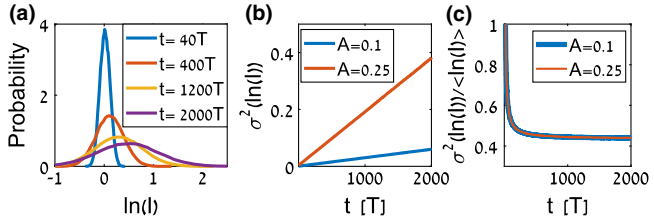

FIG. 4. (a) Histograms of the intensity logarithm at different propagation times (indicated by different colors), normalized to describe probability. All of the distributions are Gaussian shaped, and as time progresses, the Gaussians become wider, with their centers shifting to higher values, indicating a growing variance and growing mean intensity. (b) Variance of the intensity logarithm as a function of time for disorder magnitudes $A = 0.1$ (blue) and $A = 0.25$ (red), showing a variance value proportional to propagation time, exactly like in Anderson systems. (c) Ratio between the ensemble variance and mean value, as function of time, for disorder magnitude $A = 0.1$ (blue) and $A = 0.25$ (red dots). The ratio quickly converges to the same constant value, as should happen in a system with single parameter scaling.

T with modulation amplitude of 0.1, resulting in a PTC with $\varepsilon = 1.9$ and 2.1. The disorder is introduced by adding a random element of uniform distribution and $A = 0.25$ magnitude: $0.25 \times U[-1, 1]$, to the permittivity of each time segment. The simulations are carried out for $10T$ FWHM pulses, with central momentum of $k = 0.33[\Omega/c]$, just on the band edge.

Figures 3(a) and 3(b) show the band structure of this PTC without disorder (blue), displaying a band gap (between 0.35 and 0.36$[\Omega/c]$) with two band edges. Figure 3(c) presents an enlargement of the left band-edge region and displays the energy growth of each momentum component of the pulse separately (log scale, blue), rather than the total energy, to highlight the large impact of the band structure. Figure 3(c) also shows the group velocity near the band edge (red), displaying an increase into superluminal values. We emphasize that the group velocity cannot be numerically calculated for each momentum component separately, as it is derived from the motion of the pulse center of mass; but just as is the case of temporal disorder without underlying periodicity, here too, it decays exponentially to zero. Another interesting case is when the momentum spectrum of the pulse fully resides inside the band gap of the disordered PTC. In this case, the disorder reduces the band gap effects of the PTC such as the exponential growth of energy, as we further discuss in the Supplemental Material [39].

The relation to Anderson localization in 1D systems calls for analyzing additional statistical properties of the ensemble, such as the distribution and variance. It has been shown [38] that the ensemble of such systems displays a distinct statistical signature of the intensity logarithm: the distribution is always Gaussian and the variance is proportional to the evolution distance. Figure 4 presents these statistical properties for our disordered PTC. Figure 4(a) shows four histograms of the intensity logarithm conforming to four different propagation times. All the histograms are Gaussian shaped (i.e., the distribution of the intensity logarithm remains Gaussian at all times); however, as the propagation duration increases, the Gaussian distributions become wider, indicating a growing variance, and their centers shift to higher values, indicating the higher (mean) intensity. These results resemble the intensity distribution in Anderson systems with one difference-in our system, the Gaussian centers shift to higher values, while in spatial Anderson systems they always shift to lower values. Figure 4(b) shows how the variance of the intensity logarithm is proportional to the propagation time, increasing linearly, exactly like 1D spatially disordered (Anderson) systems.

These statistical features are part of the single parameter scaling theory, which explains how both the intensity mean value and distribution in Anderson systems are governed by a single parameter [38]. Both the mean exponential decay rate (Lyapunov exponent) and the ensemble variance growth rate can be derived from the same parameter. An easy way to identify single parameter scaling is a constant ratio between the mean intensity and the variance of the intensity logarithm across systems with different parameters. Figure 4(c) displays this ratio for two levels of disorder. The ratio quickly converges to a constant value of ~0.44 for both values of disorder magnitude, indicating the existence of single parameter scaling in our system.

To summarize, we studied the evolution of light pulses in disordered PTCs and found that their group velocity slows down exponentially until they all eventually stop, while their energy grows exponentially. Additionally, we studied

how the underlying band structure of disordered PTCs affects the localization, and the relation to group velocity. For the sake of generality, we used the parameter Ω to describe the modulation frequency and expressed the other important parameters of the system, such as the wave number and time (k and t) through Ω. This allows us to not limit these findings to a specific system, material, or frequency regime, but describe the general concepts and arising phenomena. Naturally, this calls for discussing the experimental feasibility of experimental observations. In the radio frequency regime, techniques for creating such temporal disorder have existed for over a decade [46], and in the optical regime, we suggest an experimental system based on epsilon-near-zero materials, with details provided in the Supplemental Material [39]. The underlying physics is closely related to Anderson localization, but has some important differences arising from the fundamental difference between spatial and temporal reflections (namely, causality prohibits time reflections from being reflected to earlier times).

This Letter suggests a new direction of research on transport phenomena in disordered PTCs, which thus far has been uncharted territory. For example, is it possible to identify Levy flights [47] in these new systems? Can these systems support hypertransport [29]? What will happen in photonic time quasicrystals? Will they support localization or enhanced transport, as happens in their spatial counterparts [48]? Undoubtedly, PTCs, with and without disorder, offer a new and exciting avenues of research. We are currently experimenting with ultrafast time-varying optical media, hoping to demonstrate photonic time crystals in the near future.

The authors acknowledge useful discussions with Prof. Boris Shapiro from the Technion. This project has received funding from the European Research Council (ERC) under the European Union's Horizon 2020 research and innovation program (grant agreement No. 789339).

*Corresponding author.
msegev@technion.ac.il

[1] PTCs are a fundamentally different phenomenon than the time crystals suggested for quantum many-body systems [F. Wilczek, Phys. Rev. Lett. **109**, 160401 (2012)], which are spontaneously emergent time periodic arising from interactions.
[2] F. R. Morgenthaler, Velocity modulation of electromagnetic waves, IRE Trans. Microwave Theory Tech. **6**, 167 (1958).
[3] D. Holberg and K. Kunz, Parametric properties of fields in a slab of time-varying permittivity, IEEE Trans. Antennas Propag. **14**, 183 (1966).
[4] J. T. M. and P. K. Shukla, Time refraction and time reflection: Two basic concepts, Phys. Scr. **65**, 160 (2002).
[5] A. B. Shvartsburg, Optics of nonstationary media, Phys. Usp. **48**, 797 (2005).
[6] V. Bacot, M. Labousse, A. Eddi, M. Fink, and E. Fort, Time reversal and holography with spacetime transformations, Nat. Phys. **12**, 972 (2016).
[7] F. Biancalana, A. Amann, A. V. Uskov, and E. P. O'Reilly, Dynamics of light propagation in spatiotemporal dielectric structures, Phys. Rev. E **75**, 046607 (2007).
[8] J. R. Zurita-Sánchez, P. Halevi, and J. C. Cervantes-González, Reflection and transmission of a wave incident on a slab with a time-periodic dielectric function $\in (T)$, Phys. Rev. A **79**, 053821 (2009).
[9] J. R. Reyes-Ayona and P. Halevi, Observation of genuine wave vector (k or β) Gap in a dynamic transmission line and temporal photonic crystals, Appl. Phys. Lett. **107**, 074101 (2015).
[10] E. Lustig, Y. Sharabi, and M. Segev, Topological aspects of photonic time crystals, Optica **5**, 1390 (2018).
[11] K. Giergiel, A. Dauphin, M. Lewenstein, J. Zakrzewski, and K. Sacha, Topological time crystals, New J. Phys. **21**, 052003 (2019).
[12] J. R. Zurita-Sánchez, J. H. Abundis-Patiño, and P. Halevi, Pulse propagation through a slab with time-periodic dielectric function $\varepsilon(T)$, Opt. Express **20**, 5586 (2012).
[13] A. Alù, M. G. Silveirinha, A. Salandrino, and N. Engheta, Epsilon-near-zero metamaterials and electromagnetic sources: Tailoring the radiation phase pattern, Phys. Rev. B **75**, 155410 (2007).
[14] M. Z. Alam, I. De Leon, and R. W. Boyd, Large optical nonlinearity of indium tin oxide in its epsilon-near-zero region, Science **352**, 795 (2016).
[15] L. Caspani, R. P. M. Kaipurath, M. Clerici, M. Ferrera, T. Roger, J. Kim, N. Kinsey, M. Pietrzyk, A. Di Falco, V. M. Shalaev, A. Boltasseva, and D. Faccio, Enhanced Nonlinear Refractive Index in ϵ-Near-Zero Materials, Phys. Rev. Lett. **116**, 233901 (2016).
[16] Y. Zhou, M. Z. Alam, M. Karimi, J. Upham, O. Reshef, C. Liu, A. E. Willner, and R. W. Boyd, Broadband frequency translation through time refraction in an epsilon-near-zero material, Nat. Commun. **11**, 1 (2020).
[17] V. Bruno, C. De Vault, S. Vezzoli, Z. Kudyshev, T. Huq, S. Mignuzzi, A. Jacassi, S. Saha, Y. D. Shah, S. A. Maier, D. R. S. Cumming, A. Boltasseva, M. Ferrera, M. Clerici, D. Faccio, R. Sapienza, and V. M. Shalaev, Negative Refraction in Time-Varying Strongly Coupled Plasmonic-Antenna-Epsilon-Near-Zero Systems, Phys. Rev. Lett. **124**, 043902 (2020).
[18] P. W. Anderson, Absence of diffusion in certain random lattices, Phys. Rev. **109**, 1492 (1958).
[19] F. K. Abdullaev and S. S. Abdullaev, On light propagation in a system of tunnel coupled waveguides, Izv. Vuz. Radiofiz **23**, 766 (1980).
[20] S. John, Strong Localization of Photons in Certain Disordered Dielectric Superlattices, Phys. Rev. Lett. **58**, 2486 (1987).
[21] H. De Raedt, A. Lagendijk, and P. de Vries, Transverse Localization of Light, Phys. Rev. Lett. **62**, 47 (1989).
[22] D. S. Wiersma, P. Bartolini, A. Lagendijk, and R. Righini, Localization of light in a disordered medium, Nature (London) **390**, 671 (1997).
[23] A. A. Chabanov, M. Stoytchev, and A. Z. Genack, Statistical signatures of photon localization, Nature (London) **404**, 850 (2000).

[24] T. Schwartz, G. Bartal, S. Fishman, and M. Segev, Transport and Anderson localization in disordered two-dimensional photonic lattices, Nature (London) **446**, 52 (2007).
[25] H. Hu, A. Strybulevych, J. H. Page, S. E. Skipetrov, and B. A. van Tiggelen, Localization of ultrasound in a three-dimensional elastic network, Nat. Phys. **4**, 945 (2008).
[26] J. Billy, V. Josse, Z. Zuo, A. Bernard, B. Hambrecht, P. Lugan, D. Clément, L. Sanchez-Palencia, P. Bouyer, and A. Aspect, Direct observation of Anderson localization of matter waves in a controlled disorder, Nature (London) **453**, 891 (2008).
[27] M. Segev, Y. Silberberg, and D. N. Christodoulides, Anderson localization of light, Nat. Photonics **7**, 197 (2013).
[28] A. M. Jayannavar and N. Kumar, Nondiffusive Quantum Transport in a Dynamically Disordered Medium, Phys. Rev. Lett. **48**, 553 (1982).
[29] L. Levi, Y. Krivolapov, S. Fishman, and M. Segev, Hyper-transport of light and stochastic acceleration by evolving disorder, Nat. Phys. **8**, 912 (2012).
[30] Y. Krivolapov, L. Levi, S. Fishman, M. Segev, and M. Wilkinson, Super-diffusion in optical realizations of Anderson localization, New J. Phys. **14**, 043047 (2012).
[31] M. Mierzejewski, K. Giergiel, and K. Sacha, Many-body localization caused by temporal disorder, Phys. Rev. B **96** 140201 (2017).
[32] D. Delande, L. Morales-Molina, and K. Sacha, Three-Dimensional Localized-Delocalized Anderson Transition in the Time Domain, Phys. Rev. Lett. **119**, 230404 (2017).
[33] H. H. Sheinfux, S. Schindler, Y. Lumer, and M. Segev, Recasting Hamiltonians with gauged-driving, in 2017 Conference on Lasers and Electro-Optics, *CLEO 2017, Proceedings*, Vol. 2017 (IEEE, New York, 2017), pp. 1–2.
[34] Y. Sharabi, E. Lustig, and M. Segev, Light propagation in temporally disordered media, in *Conference on Lasers and Electro-Optics* (The Optical Society, 2019), p. FF3B.1.
[35] J. Mendonça, *Theory of Photon Acceleration* (CRC Press, Boca Raton, FL, 2000).
[36] Notice that $Z_i = D_i/B_i = \sqrt{\varepsilon_i/\mu_i}$, the inverse of the usual wave impedance in a medium, defined as $\eta_i = E_i/H_i = \sqrt{\mu_i/\varepsilon_i}$.
[37] Y. Lahini, A. Avidan, F. Pozzi, M. Sorel, R. Morandotti, D. N. Christodoulides, and Y. Silberberg, Anderson Localization and Nonlinearity in One-Dimensional Disordered Photonic Lattices, Phys. Rev. Lett. **100**, 013906 (2008).
[38] L. I. Deych, A. A. Lisyansky, and B. L. Altshuler, Single Parameter Scaling in One-Dimensional Localization Revisited, Phys. Rev. Lett. **84**, 2678 (2000).
[39] See Supplemental Material at http://link.aps.org/supplemental/10.1103/PhysRevLett.126.163902 for additional information and explanations about pulse propagation in band gaps, continuous temporal disorder, and possible experimental platforms, which include Refs. [40–45].
[40] M. Rechtsman, A. Szameit, F. Dreisow, M. Heinrich, R. Keil, S. Nolte, and M. Segev, Amorphous Photonic Lattices: Band Gaps, Effective Mass, and Suppressed Transport, Phys. Rev. Lett. **106**, 193904 (2011).
[41] H. Herzig Sheinfux, I. Kaminer, A. Z. Genack, and M. Segev, Interplay between evanescence and disorder in deep subwavelength photonic structures, Nat. Commun. **7**, 12927 (2016).
[42] E. Gurevich and O. Kenneth, Lyapunov exponent for the laser speckle potential: A weak disorder expansion, Phys. Rev. A **79**, 063617 (2009).
[43] P. Lugan, A. Aspect, L. Sanchez-Palencia, D. Delande, B. Grémaud, C. A. Müller, and C. Miniatura, One-dimensional Anderson localization in certain correlated random potentials, Phys. Rev. A **80**, 023605 (2009).
[44] A. Dikopoltsev, H. Herzig Sheinfux, and M. Segev, Localization by virtual transitions in correlated disorder, Phys. Rev. B **100**, 140202(R) (2019).
[45] E. Lustig, S. Saha, E. Bordo, C. DeVault, S. N. Chowdhury, Y. Sharabi, A. Boltasseva, O. Cohen, V. M. Shalaev, and M. Segev, Towards photonic time-crystals: Observation of a femtosecond time-boundary in the refractive index, CLEO 2021 (2021).
[46] J. R. Zurita-Sánchez and P. Halevi, Resonances in the optical response of a slab with time-periodic dielectric function $\varepsilon(T)$, Phys. Rev. A **81**, 053834 (2010).
[47] P. Barthelemy, J. Bertolotti, and D. S. Wiersma, A Lévy flight for light, Nature (London) **453**, 495 (2008).
[48] L. Levi, M. Rechtsman, B. Freedman, T. Schwartz, O. Manela, and M. Segev, Disorder-enhanced transport in photonic quasicrystals, Science **332**, 1541 (2011).